Ice wastage on the Kerguelen Islands (49°S, 69°E) between 1963 and 2006

Etienne Berthier, Raymond Le Bris, Laure Mabileau, L. Testut, Frédérique
Rémy

Ice wastage on the Kerguelen Islands (49°S, 69°E) between 1963 and 2006.

Berthier E.[1], Le Bris R.[2], Mabileau L.[1], Testut L.[3] & Rémy F.[1]*

[1] LEGOS, CNRS, 14 avenue Edouard Belin, F-31400 Toulouse, CEDEX 9, France.

[2] Department of Geography, University of Zurich, Winterthurerstrasse 190, CH-8057 Zurich, Switzerland.

[3] Université de Toulouse; UPS (OMP-PCA); LEGOS; 14 Av. Edouard Belin, F-31400 Toulouse, France.

* corresponding author etienne.berthier@legos.obs-mip.fr

Abstract

We observed the wastage of ice masses on the Kerguelen Islands (Indian Ocean, 49°S, 69°E) using historical information and recent satellite data. Overall, the total ice-covered area on the islands declined from 703 to 552 km^2 between 1963 and 2001, a reduction of 21%. The area of Cook ice cap (the main ice body) decreased asymmetrically from 501 to 403 km^2. West-flowing glaciers lost 11% of their area while east-flowing glaciers lost 28%. After 1991, the retreat rate accelerated from 1.9 km^2/yr (1963-1991) to 3.8 km^2/yr (1991-2003). Between 1963 and 2000, the ice volume loss was 25-30 km^3, equivalent to an area-average ice thinning rate of 1.4-1.7 m/yr. The glacial retreat took place in the climatic context of a relatively low level of precipitation (compared to the 1950s) and a ~1°C warming that occurred between 1964 and 1982. The acceleration of the ice losses since, at least, the 1990s indicates that the state of the ice bodies on the Kerguelen Islands is still far from balanced. Together with other studies in Patagonia, South Georgia and Heard Island, our analysis is consistent with a pattern of strong and accelerated wastage of ice masses influenced by the Southern Ocean.

Keywords

I. Introduction

The Kerguelen Islands (49°S, 69°E) are a group (7215 km^2) of isolated islands in the southern Indian Ocean that were 10% ice-covered in 1963. The French TAAF (*Terres Australes et Antarctiques Françaises*) organized several scientific missions to the islands between 1961 and 1966, nearly two centuries after their discovery by Yves de Kerguelen in 1772. Approximately 5000 aerial photographs were taken of the three main glacierized areas: Cook ice cap, Rallier du Baty Peninsula and Mount Ross (highest peak at 1850 m a.s.l., Figure 1). One outcome was a comprehensive map of the islands published by Institut Géographique National (IGN) [1967] (hereinafter referred to as the IGN map) [see also *Durand de Corbiac*, 1970].
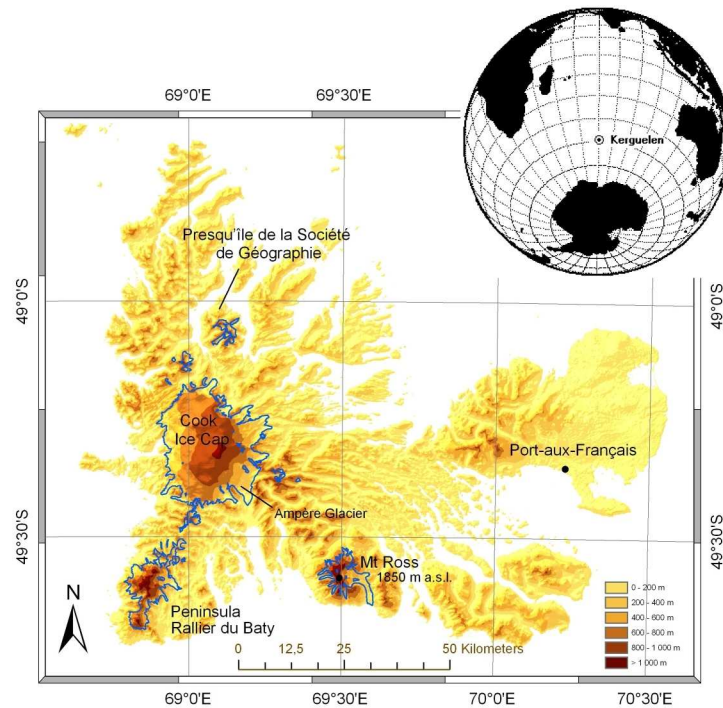

Figure 1: Topography of Kerguelen Islands. The four main glacierized areas and the base station (Port-aux-Français) are indicated. The small globe identifies the Islands in the South Indian Ocean.

These early measurements were followed by several glaciological field campaigns in the early 1970s. Ampère glacier, a southern outlet that drained one fifth of Cook ice cap, was the main target of these surveys. A map of the sub-glacial topography was made [*Vallon*, 1977b] and some measurements of the mass and energy balance and the surface elevation changes were performed [*Poggi*, 1977; *Vallon*, 1977a]. Aerial photographs taken in February 1974 were used to derive a detailed topographic map covering most of the ablation area of the Ampère and neighboring Diosaz glaciers. Vallon [1977a] observed that, in the 1960s and the early 1970s, Ampère glacier was rapidly receding and thinning.

Ice masses on the Kerguelen Islands belong to a group of ice caps and glaciers located on sub-Antarctic islands, covering a total area of ~7000 km^2 [*Dyurgerov and Meier*, 2005]. Multi-decadal measurements of glacier changes are rare on these sub-Antarctic islands [*Dyurgerov and Meier*, 2005; *Cogley*, 2009]. Thus, the objective of the present study is to combine the available historical information on the Kerguelen Islands with modern satellite data to inventory all ice masses and assess their evolution during the last four decades in the context of climate records at Port-aux-

Français (Figure 1). Glacier fluctuations are also compared to those reported for other ice masses around the Southern Ocean.

II. Changes in ice-covered areas

II.1. Data and Methods

We measured the extent of glaciers and ice caps on the Kerguelen Islands by digitizing and comparing successive glacier outlines on a map and satellite images. Our oldest data set is the map published by IGN at a scale of 1:200,000. It was produced using aerial photographs taken in 1963 of Cook ice cap and in 1964 of Presqu'île de la Société de Géographie, Mount Ross and Rallier du Baty Peninsula (M. Vallon, personal communication, 2008). The IGN map was reprojected from UTM-International Ellipsoid to UTM-WGS84.

For Cook ice cap, the main ice body, a comprehensive collection of optical images was compiled to provide a time series of ice cap extent. SPOT (1991, 1994 and 2003), Landsat (November 2001) and Advanced Spaceborne Thermal Emission and reflection Radiometer (ASTER; 2005 and 2006) images are listed in Table 1. For ice masses other than Cook ice cap, glacier outlines were derived from only one recent (SPOT 1994 or Landsat 2001) satellite image, in addition to the IGN map. Both glacier inventories (for 1963-64 and 1994-2001) have been incorporated into the Global Land Ice Measurements from Space (GLIMS) Glacier Database (http://nsidc.org/glims/).

Satellite	Date	Id (reference number)
SPOT 2	1991-09-08	22324509109080507162P
SPOT 3	1994-03-03	32324509403030522061P
SPOT 5	2003-11-16	52324500311160538041A
Aster	2005-02-14	SC:AST_L1A.003:2028170903
Aster	2006-01-11	SC:AST_L1A.003:2032694112
Landsat	2001-01-11	LE71390942001011SGS00 (source Global Land Cover Facility)
Landsat	2001-03-09	LE71380952001068SGS00 (source Global Land Cover Facility)
Landsat	2001-11-27	LE71390942001331SGS00 (source Eurimage)

Table 1: Satellite images used in this study. Dates are given as YYYY-MM-DD. Pixel sizes are 2.5 m for Spot-5; 10 m for Spot-2 and Spot-3; 15 m for Aster and Landsat images.

Due to its coarse scale (1:200,000), the IGN map is not a suitable source of ground control points for orthorectifying high resolution satellite images. Instead, we chose a Landsat-7 panchromatic image acquired 11 January 2001 (orthorectified through the Global Land Cover Facility –GLCF-project, http://glcf.umiacs.umd.edu/index.shtml) as a reference; all other data (map and satellite images) were co-registered to this reference. Thus, the absolute location of all our data may not be perfect (±50 m according to the GLFC webpage); however, this does not have a major impact on the relative changes in ice-covered areas. The choice of a Landsat image as a reference was motivated by its large footprint (180 km by 180 km), which allows most ice masses to be included in a single image.

SPOT and Aster (Level 1A) images were orthorectified and co-registered to the Landsat scene using the COSI-CORR software [*Leprince et al.*, 2007] and the SRTM (Shuttle Radar Topographic Mission) DEM.

The accuracy of the co-registration of the IGN map and satellite images to the Landsat scene was assessed by comparing the cartographic coordinates of 20 to 25 points that could be identified on the map and satellite images (lakes, mountain peaks, etc). Satellite images are co-registered within one or two pixels of the Landsat reference image (Table 2). In the case of the IGN map, errors are about ±100 m in both directions, leading to a relatively large uncertainty (±140 m) for the position of glacier outlines.

Data	Year	Std deviation X (m)	Std deviation Y (m)
IGN	1963-64	114.7	105.9
SPOT	1991	8.5	6.7
	1994	13.3	6.0
	2003	8.4	12.0
Landsat	2001-03	22.4	12.3
Landsat	2001-11	8.4	11.7
Aster	2005	38.7	14.9
	2006	23.4	14.4

Table 2: Relative horizontal accuracy between the different data sets and the reference 11 January 2001 Landsat image.

Another source of uncertainty is the ability of the operator to identify the glacier outline on the map and on the satellite images, i.e. an outline pointing error. Human interpretation probably remains the best means for extracting consistent glacier outlines from different data sets [*Raup et al.*, 2007]. To ensure consistency of the successive outlines, any given ice body was always digitized by the same operator. Two operators independently digitized the same ice body and an "outline pointing" of about ±1 pixel was determined.

The co-registration error and the "outline pointing" error were summed quadratically to estimate the total error. A conservative estimate of the error for the ice extent was then obtained by multiplying this total error by the perimeter of each ice body [*Rivera et al.*, 2007].

II.2. Retreat of all glaciers and ice caps

Region	Year	Area (km^2)	Ice loss, km^2 (%)
Cook ice cap	1963	500.9	90.9 (*18.2*)
	2001	410.0	
Rallier du Baty Peninsula	1964	102.3	23.1 (*22.5*)
	2001	79.2	
Mont Ross	1964	59.3	24.2 (*40.8*)
	2001	35.1	
Presqu'île de la Société de Géographie	1964	14.7	10 (*68*)
	1994	4.7	

Table 3: Changes in ice-covered areas between 1963-64 and 2001 (1994 for Presqu'île de la Société de Géographie). The ice losses (in km^2 and in percentage of the initial surface) are given in the last column. Isolated glaciers (covering 18 km^2 in 1963-1964) are not included in this table.

In 1963/64, the total ice-covered area on the Kerguelen Islands was 703±51 km^2. Our inventory is consistent with another analysis (based on the same input data) that found a total glacier extent of

698 km^2 (J. G. Cogley, personal communication, 2008). The areal changes for the four main glacierized regions on the Kerguelen Islands are summarized in Table 3. Between 1963-64 and 2001, the ice-covered areas on Cook ice cap, Rallier du Baty Peninsula and Mont Ross contracted from 662±45 km^2 to 524±10 km^2, a reduction of 21%. The relative ice loss is massive for Presqu'île de la Société de Géographie, the glacierized area of which contracted from 14.7±1 km^2 in 1964 to 4.7±0.1km^2 in 1994. For this small region, if this rate of shrinkage (0.33 ± 0.03 km^2/a) remained unchanged since 1994, the glaciers should have disappeared in 2008 or 2009. In 2001, the total ice-covered area on the Kerguelen Islands shrank to 552±11 km^2.

II.3. Accelerating and asymmetrical retreat of Cook ice cap

Due to clouds in the images, complete glacier outlines for Cook ice cap were available only in 1963, 2001 and 2003. However, in 1991 only a small fraction (5%) of the ice cap was masked by clouds. Hence, for this small fraction, we computed the ice extent by linear interpolation between the 1963 and 2001 outlines.

Between 1963 and 2001, the size of Cook ice cap decreased from 501 km^2 to 410 km^2 (Figure 2a). This reduction is due to the strong retreat of all outlet glacier fronts and the growth and appearance of nunataks (isolated rock outcrops within the ice cap). We estimated the overall rate of contraction for two time periods (Figure 2b). The ice loss was 1.9±1.3 km^2/yr between 1963 and 1991 and increased to 3.8±0.7 km^2/yr after 1991. Thus, in recent years, nearly 1% of the ice cap has disappeared annually. The temporal resolution of our data on glacier change is rather low and does not permit us to observe the inter-annual or decadal variability of the ice loss. However, we detect a recent acceleration of ice loss.
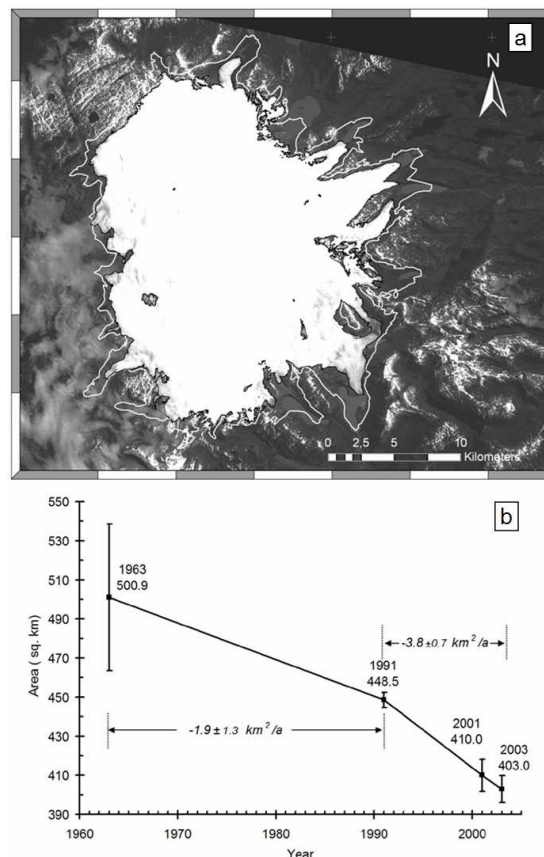

Figure 2: Retreat of Cook ice cap between 1963 and 2001. (a) 2001 Landsat image with the 1963 (white) and 2001 (black) glacier outlines. (b) Temporal changes of the ice-covered area. The rates of glacier shrinkage (km^2/yr) are indicated for 1963-1991 and 1991-2003.

The retreat also exhibits a strong asymmetry between the eastern and western sides. To quantify this difference, we examined changes on either side of the ice divide which formed the boundary between two nearly-identical sectors of Cook ice cap, covering ~250 km^2 each in 1963 (Figure 3). The area of the western part contracted from 255±19.1 km^2 to 226±3.8 km^2 between 1963 and 2003, losing ~11%. The eastern part lost ~28% of its initial surface, from 247±18.5 km^2 to 177±3.0 km^2. Thus, the shrinkage was 2.5 times greater in the east than in the west. This conclusion also holds if 1963-2003 is split into two time periods: 1963-1991 and 1991-2003 (Table 4). The asymmetry of the retreat is a continuous feature throughout the last 40 years.
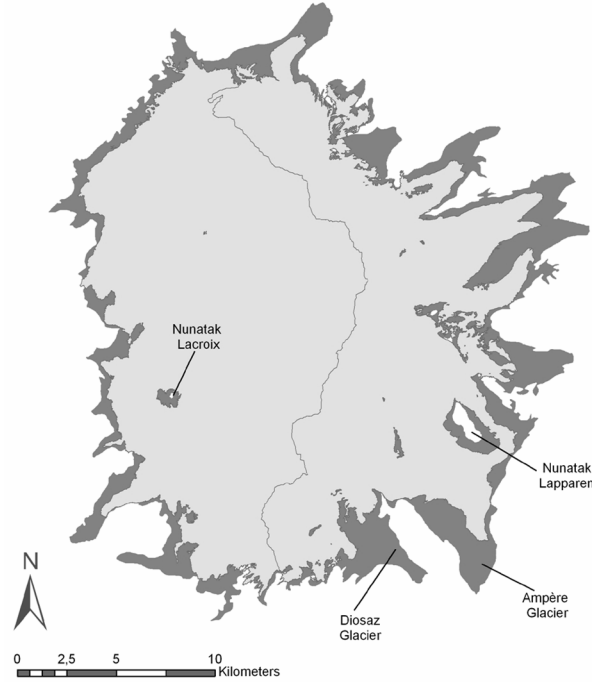

Figure 3: East/west asymmetry of Cook ice cap shrinkage. The dark grey represents ice-covered areas that disappeared between 1963 and 2001.

	1963 area	1991 area	Ice loss, km^2 (%)	Rate of Ice loss, km^2/yr
East	246.9 ± 18.5	210.3 ± 1.8	36.6 (*14.8*)	1.3
West	254.9 ± 19.1	236.4 ± 2.0	18.5 (*7.2*)	0.7
	1991 area	**2003 area**	**Ice loss, km^2 (%)**	**Rate of Ice loss, km^2/yr**
East	210.3 ± 1.8	177.3 ± 3.0	33.0 (*15.7*)	2.8
West	236.4 ± 2.0	225.8 ± 3.8	10.6 (*4.5*)	0.9
	1963 area	**2003 area**	**Ice loss, km^2 (%)**	**Rate of Ice loss, km^2/yr**
East	246.9 ± 18.5	177.3 ± 3.0	69.6 (*28.2*)	1.7
West	254.9 ± 19.1	225.8 ± 3.8	29.2 (*11.4*)	0.7

Table 4: Evolution of the ice-covered areas (km^2) in 1963, 1991 and 2003 for the eastern and western parts of Cook ice cap (in parenthesis, the percentage of the initial surface that has been lost).

II.4. Retreat of Ampère glacier

To study the behavior of each outlet glacier, Cook ice cap was split into different drainage basins using the SRTM DEM (Figure 4a, inset). We discuss here the evolution of the largest and best studied [*Vallon*, 1977b; a; *Frenot et al.*, 1993] outlet glacier, Ampère glacier.

The successive glacier outlines are plotted in Figure 4a. Between 1963 and 2006, the retreat of the terminus was 2830±161 m, equivalent to a mean retreat rate of 70±3.7 m/yr, the glacier length decreased from 15.3 km to 12.5 km and the glacier contracted by 18.3±5.1 km^2 (Figure 4b). The area loss took place mostly close to the glacier front, where a proglacial lake (Ampère Lake) appeared in the 1960s and covered 1.6 km^2 in 1991 and 3.5 km^2 in 2006.
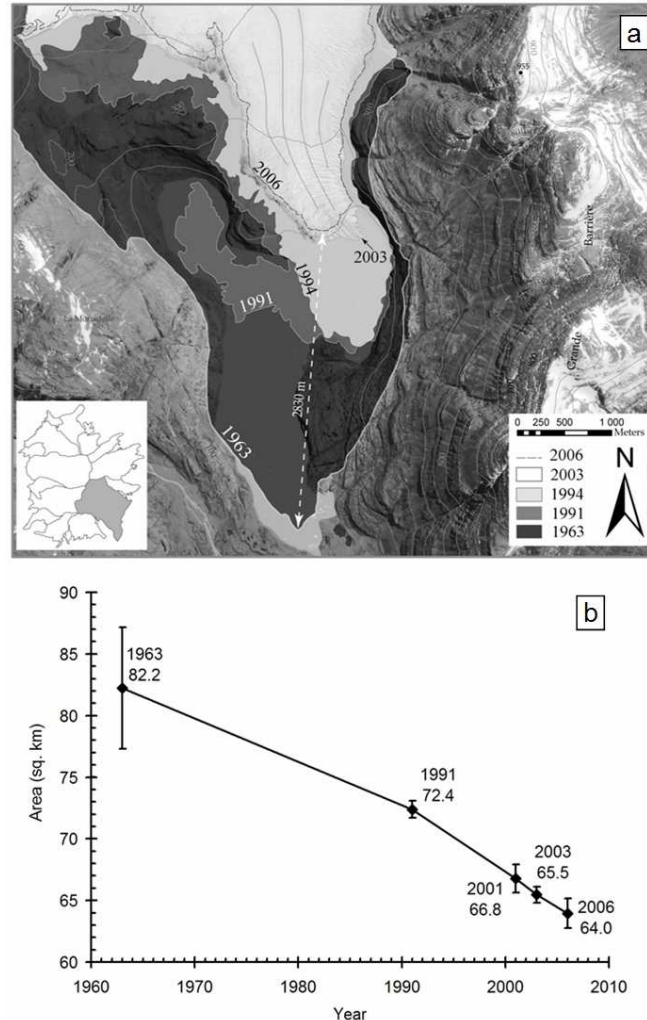
Figure 4: Shrinkage of Ampère glacier between 1963 and 2006. (a) Retreat of the glacier front. (b) Temporal changes of the ice-covered area.

III. Changes in ice volume

III.1. Elevation datasets

III.1.a. 1963-IGN map

To assess the vertical accuracy of the IGN map, we compared the altitudes of 43 geodetic points located in ice-free regions with the elevations from the SRTM DEM. The standard deviation (SD) of the elevation differences was 19.4 m. Given the ±4 m error of the SRTM DEM (error at 1 SD, see below), a ±19 m uncertainty was attributed to the 1963 Cook ice cap elevations below 700 m a.s.l. (~300 km^2 in 1963). No significant elevation bias was observed.

However, the altitudes in the central part of Cook ice cap (above 700 m a.s.l. and covering 200 km^2 in 1963) must be considered with caution since the 1963 aerial photographs were acquired only within a distance of 3 km from the ice cap margin [*Vallon*, 1977a] and the contour lines in the interior were drawn manually. Yet, Vallon [1977a] pointed out the good quality of the map in the accumulation area and never found errors larger than "a few tens of meters". Thus, we used a conservative systematic error of ±50 m in the central part of the ice cap.

III.1.b. 1974 map

The 1974-map encompasses 36 km^2 of ice-covered areas. Most of it (31 km^2) corresponds to the lowest 40 % of Ampère glacier; the rest consists of Diosaz glacier. The map was published in a local coordinate system [*Vallon*, 1977a]. The map was co-registered to the SRTM DEM by collecting tie points on the two elevation contour maps. We then digitized the 1974 elevation contours and converted them into a continuous surface (a DEM) using the PCI Orthoengine^{SE} software (version 10). The registration between the SRTM and 1974-map was found to be within ±150 m. This relatively large co-registration error is not due solely to errors in the 1974-map but also reflects the difficulty of co-registering two elevation datasets with a coarse resolution (posting of 90 m for the SRTM DEM).

The vertical accuracy of the 1974-map was assessed on the stable terrain surrounding the glaciers. On average, the map was 10 m lower than the SRTM DEM. This systematic difference was added to the 1974 DEM values. Locally, the elevation differences can be much larger on the steep non-glacierized slopes surrounding the tongue of Ampère glacier, a result of the difficulty of co-registering the two elevation datasets. The standard deviation of the elevation difference on this steep ice-free terrain is 25 m and provides a conservative estimate of the elevation difference errors on the smoother topography of Ampère and Diosaz glacier tongues.

III.1.c. SRTM DEM and ICESat elevation profiles

The shuttle radar topographic mission (SRTM) was flown in February 2000 [*Rabus et al.*, 2003]. The SRTM DEM of Kerguelen Islands, downloaded from ftp://e0srp01u.ecs.nasa.gov (SRTM3, version 2), is characterized by a small percentage of data voids (~1%). Although SRTM is a global product, previous studies reported some significant regional differences in its accuracy [*Berthier et al.*, 2006; *Rodriguez et al.*, 2006; *Surazakov and Aizen*, 2006]. Thus, SRTM errors need to be determined on stable ice-free land before any glaciological application.

The SRTM DEM was evaluated against ICESat data obtained from the National Snow and Ice Data Center [*Zwally et al.*, 2002]. We used GLAS release 28 (GLA14 product) and collected all the laser periods available at the time of our study (laser period 1A to 3H from February 2003 to March 2007, Figure 5a). For each laser footprint (covering about 70 m), the corresponding SRTM elevation is extracted by bilinear interpolation. All ICESat data points for which the elevation difference with SRTM was greater than 50 m were considered outliers and removed [*Carabajal and Harding*, 2005]. They correspond to reflections at the top of clouds. The histogram of the elevation differences between SRTM and ICESat for the remaining points is shown in Figure 5b. This comparison underlines the remarkable accuracy of the SRTM DEM on Kerguelen Islands, which exhibits a very small bias (SRTM lower than ICESat only by 0.2 m, SD = 4.1; n=6676).
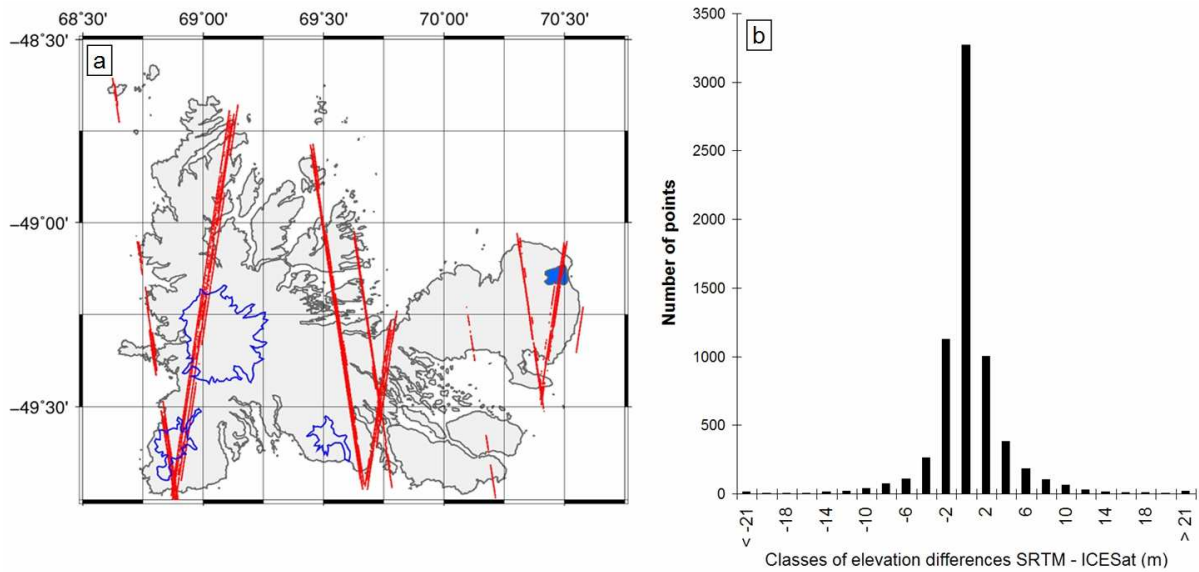
Figure 5: Comparison of SRTM and ICESat elevations. (a) Location of all ICESat laser footprints available between 2003 and 2007. (b) Distribution of the elevation differences on ice-free terrain. The mean difference is 0.2 m (standard deviation = 4.1 m; n=6776).

Penetration of the C-Band radar signal in dry snow at high elevations has been shown to be significant in Greenland and Alaska and could lead to underestimated SRTM elevations in the upper accumulation regions of glaciers [*Dall et al.*, 2001; *Rignot et al.*, 2001]. However, in the case of Kerguelen Islands, February 2000 was one of the warmest months ever recorded (with a mean temperature of 9.1°C at Port-aux-Français, 35 m a.s.l.). Thus, if we assume a strong (dry) adiabatic lapse rate of -10 K/km, even the highest point on the ice cap (1040 m a.s.l.) probably experienced some melting in February 2000. Hence, C-Band penetration must have minimal impact on the SRTM elevations. Consequently, the SRTM DEM appears to be an excellent reference topographic dataset for mapping ice elevation changes.

III.2. Ice elevation changes

III.2.a. 1974-2000 elevation changes on the Ampère and Diosaz glaciers

By subtracting the 1974 DEM from the 2000 DEM, we calculated the 26-year elevation difference for the Ampère and Diosaz glaciers. It is a minimum estimate of the ice thinning, as it does not take into account the ice that was replaced by water in Ampère and Diosaz lakes. The bathymetry of these lakes is not known. Ampère glacier bedrock, measured in the 1970s [*Vallon*, 1977b], reached 100 m below sea level close to the glacier front where Ampère lake had, in 2000, an altitude of 25 m a.s.l. This suggests a maximum underestimation by 125 m for the ice thinning. Note that the area where bedrock was below Ampère Lake level in 2000 (and thus where ice thinning is underestimated) covers less than ~2 km^2.

All ice-covered areas have thinned since 1974 (Figure 6). On Ampère glacier, the maximum thinning reaches, at least, 220±25 m (8.5±0.9 m/yr) in regions that are now fully deglacierized and filled by Ampère Lake. The disintegration is even more spectacular at the tongue of Diosaz glacier, which thinned by over 330±25 m. The higher thinning rates (12.7±0.9 m/yr) for Diosaz glacier are probably due to a local high point in its bedrock topography: a small initial thinning in the 1960s at this location greatly reduced the ice fluxes toward the downstream glacier tongue, which then disintegrated rapidly (M. Vallon, personal communication, 2008). On average, the lowering of the glacier surfaces has been 115±25 m (4.4±0.9 m/yr).
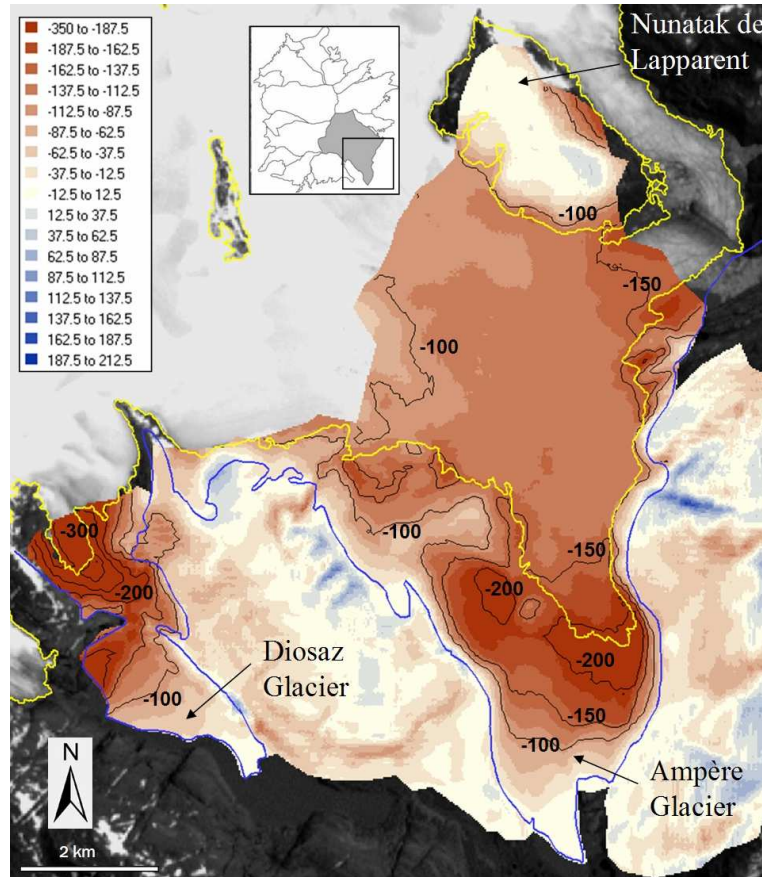
Figure 6: Ampère glacier elevation changes between 1974 and 2000 measured by comparing the SRTM DEM with a map [Vallon, 1977a]. The glacier outlines in 1974 (blue) and 2000 (yellow) and the -100, -150, -200, -250 and -300 m elevation differences (thin black line) are shown.

III.2.b. 1963-2000 elevation changes around nunataks

We use the 1963-IGN map and 2001-Landsat image to determine the growth of nunataks and derive elevation changes from a single elevation dataset (here the SRTM DEM). Growing rock outcrops have been used as a qualitative indicator of glacier downwasting in the Alps and Patagonia [*Paul et al.*, 2007; *Rivera et al.*, 2007]. Here, they are used quantitatively to determine ice thinning.

The principle of the technique is illustrated in Figure 7a, a 3D-view of nunatak Lapparent, on the eastern side of Ampère glacier. The outlines of the nunatak in 1963 and 2001, overlaid on the 2003 Spot-5 image, show its significant growth (from 0.99 to 3.45 km^2) due to the lowering of the glacier surface. Because nunatak Lapparent covers a large elevation range (from 400 to 600 m a.s.l.) experiencing different thinning rates, it was divided into 3 parts using transects parallel to elevation contours on the surrounding ice cap. For each part, the elevation drop was computed by subtracting the mean SRTM elevation along the 1963 outline from the mean SRTM elevation along the 2001 outline. Elevation change uncertainty is due to a geolocation (horizontal) error of the nunatak margin in the 1963-IGN map and 2001-Landsat image. It is calculated as the product of the horizontal error of each glacier outline (Table 2) and the tangent of the slope angle in the vicinity of the outline [*Echelmeyer et al.*, 1996].

The agreement between the thinning measured on each side of nunatak Lapparent (within a few meters) gives some confidence in our method (Figure 7b). The ice losses were largest at the lowest elevations. The thinning rates were 3.5±1.6 m/yr at 600 m a.s.l., 4.8±1.6 m/yr at 500 m a.s.l. and 5.9±1.6 m/yr at 400 m a.s.l.
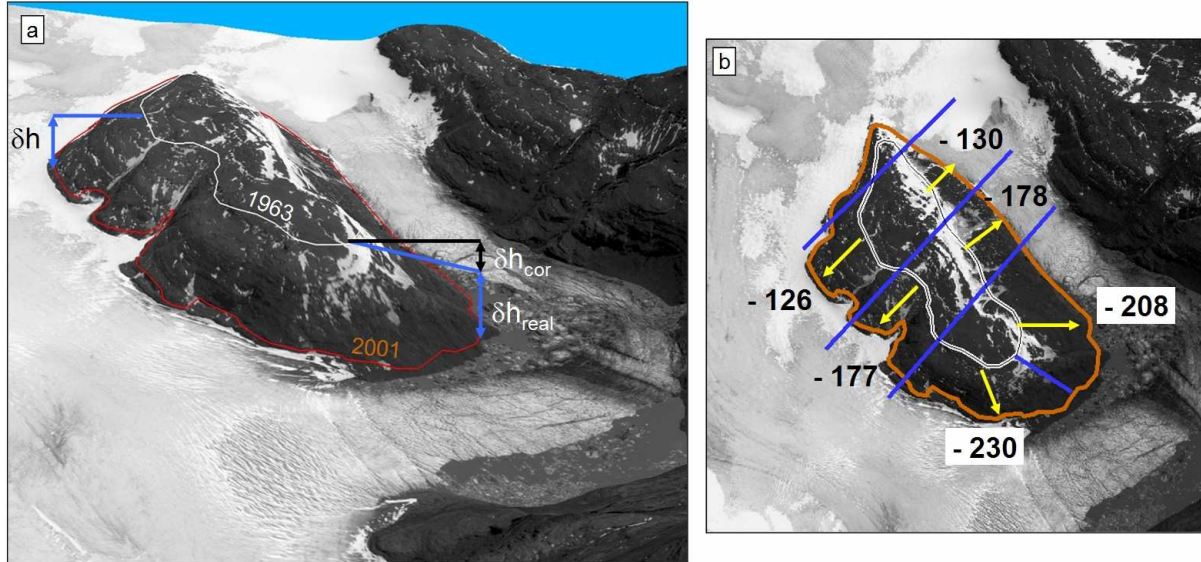

Figure 7: Growing nunataks as indicators of ice elevation changes. (a) 3D view of nunatak Lapparent (region of Ampère glacier, Figure 3) with its outline in 1963 (white) and 2001 (red). The blue arrows symbolize the thinning that can be measured using a single topography (here, SRTM). In the lowest parts of the nunatak, real elevation changes (noted δh_{real}) were obtained after applying a ~50 m correction (symbolized by a black arrow and noted δh_{cor}) to take into account the non horizontal slope of the 1963 ice surface. (b) Mean ice elevation changes around nunatak Lapparent between 1963 and 2000.

Our method only works if nunataks were already present in the oldest map (here 1963); otherwise it would only provide a minimum estimate of the ice thinning. Apart from nunatak Lapparent, only nunatak Lacroix, on the western side of Cook ice cap, was also visible in 1963. The altitude of nunatak Lacroix is only slightly higher (650 m a.s.l.) than the highest part of nunatak Lapparent, but the thinning rate (1.3±0.8 m/yr) was 2.4 times less.

III.2.c. 2000-2005 elevation changes on Rallier du Baty Peninsula

Due to clouds, the only ICESat profile useful for measuring ice elevation changes was acquired 25 February 2005 across Arago glacier, a western outlet of Rallier du Baty Peninsula ice cap (Figure 8). The elevation differences are small outside the glacier, confirming the consistency of the SRTM and ICESat elevations. A clear lowering of the glacier surface is observed during the five years separating the two surveys (2000-2005), both performed in February so that seasonal effects have little impacts on these elevation changes. The mean lowering was 30.5±4.1 m (6.1±0.8 m/yr). This single profile confirms the potential of combining ICESat profiles and SRTM DEM to map glacier elevation changes [*Surazakov and Aizen*, 2006]. The main limitations are the limited amount of cloud-free ICESat data and the spacing of the different tracks.
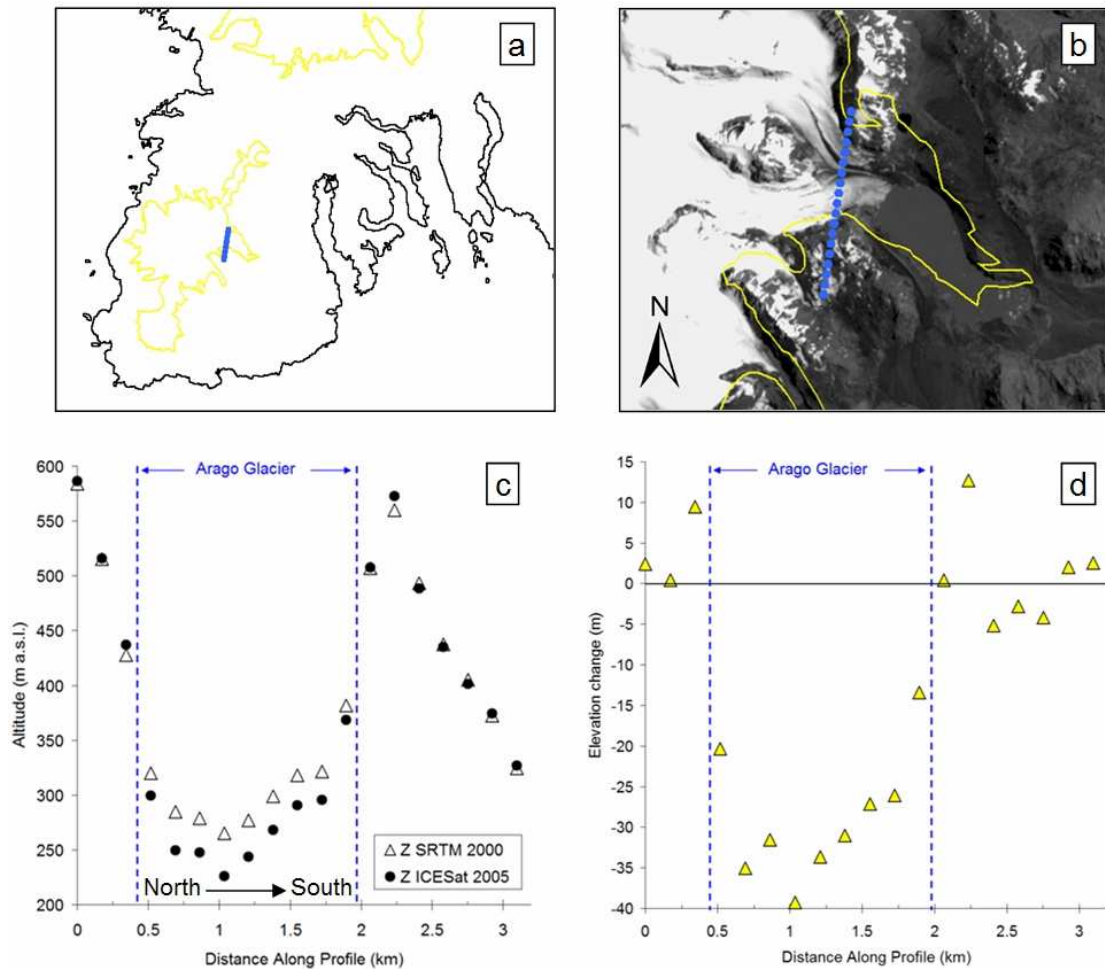
Figure 8. Recent (2000–2005) elevation changes on Rallier du Baty Peninsula (Figure 1). (a) Location of the 25 February 2005 ICESat track (laser period 3B) across Arago glacier; in yellow, the glacier limit in 1964; (b) close-up, background is a 2001 Landsat image; (c) elevation profile extracted from the SRTM DEM and ICESat; (d) elevation changes between February 2000 and February 2005.

For the same profile on Arago glacier, we also extracted the mean elevation from the 1964-IGN map. Between 1964 and 2000, the surface lowering was 80±19 m (from 375 to 295 m a.s.l.), equivalent to a mean thinning rate of 2.2±0.5 m/yr. This is another indication that ice losses have accelerated during recent years.

III.3. Cook ice cap total volume change

III.3.a. Volume change using sequential DEMs

The 37-year volume change of Cook ice cap is calculated by subtracting the 1963-IGN map from the 2000-SRTM DEM. The elevation differences range from -400±19 m (maximum thinning for Diosaz glacier) to 50±50 m (at high elevations on the western side of Cook ice cap). We have no means of assessing whether the thickening in the accumulation area is a realistic feature. Rather, the appearance of small nunataks at elevations as high as 800 m a.s.l. suggests that the thickening is an artifact due to large errors in the IGN map. Consequently, our volume loss may be underestimated. By summing the elevation changes over all grid cells, we found a total ice loss of 26.4±15.9 km^3 over 37 years. The ice losses were 3.4 times larger on the eastern side than on the

western side. The latter observation is in agreement with our findings of rapidly growing nunataks and stronger glacier retreat on the eastern side.

III.3.b. Volume change by extrapolating local elevation changes

All measured elevation changes were compiled as a function of altitude (Figure 9). The sharp reduction in thinning at the lowest elevations for the Diosaz and Ampère glaciers is due to the disappearance of all the ice that existed at the terminus, leaving unchanging bedrock or water.
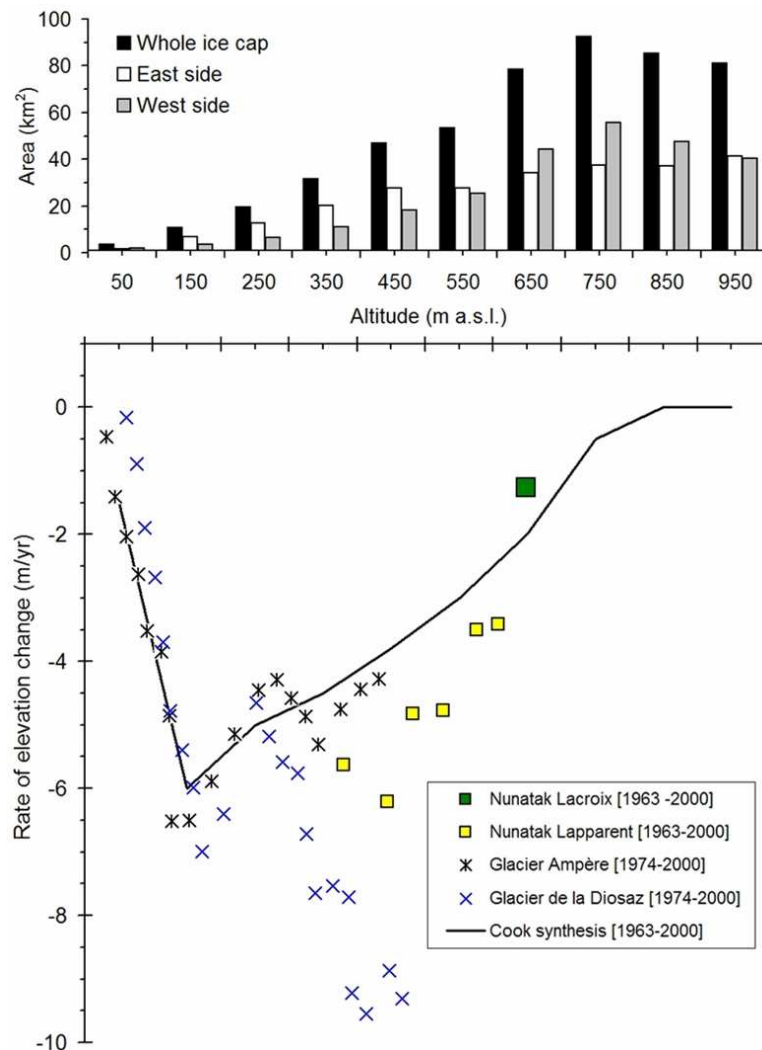

Figure 9: Hypsometry of Cook ice cap in 1963 (upper panel) and elevation changes as a function of altitude on different regions of the ice cap (lower panel). The elevation differences were measured by comparing two topographies (1974-2000, Figure 6) and analyzing the growth of nunataks (1963-2000, Figure 7).

These ice elevation changes were combined with the 1963 hypsometry of Cook ice cap to obtain another estimate of its ice volume loss. We first synthesized our sparse and inhomogeneous measurements of ice thinning rates into a generic curve. In computing this curve, we did not take into account the very high thinning rates on Diosaz glacier or around the lower reaches of nunatak Lapparent, as they are due to local destabilizing effects (e.g. disintegration of glacier tongues calving into lakes). We assumed that the 1974-2000 elevation changes for Ampère glacier are representative of all ice-covered areas lying between sea level and 450 m a.s.l. Between 600 and 700 m a.s.l., we calculated the average of the elevation changes measured around the nunatak Lacroix (in the west) and the upper reaches of nunatak Lapparent (in the east). Linear interpolation

was used between 450 and 600 m a.s.l. We do not have any measurement of elevation changes above 700 m a.s.l. We assumed a limited thinning between 700 and 800 m a.s.l. (0.5 m/yr) and no elevation change above 800 m a.s.l. The occurrence of thinning between 700 and 800 m a.s.l. is supported by the emergence of new, but still small, nunataks on recent satellite images (both in the eastern and western side of the ice cap). Also, we implicitly assumed that the rates of elevation changes for 1963-2000 and 1974-2000 were identical. This assumption is supported by the observation of fast thinning on Ampère glacier (8 to 10 m/yr below 200 m a.s.l.) between 1962 and 1974 [*Vallon*, 1977a]. This curve is labeled "Cook synthesis" in Figure 9 and, combined with the hypsometry, leads to an ice loss of 29.8 km^3.

III.3.c. Volume change using a scaling relationship

The size of Cook ice cap decreased from 501 km^2 in 1963 to 410 km^2 in 2001. Area changes are converted to volume changes using an empirical scaling relationship derived from six ice sheets and ice caps that were "sounded in enough detail to make volume estimates" [*Paterson*, 1972]:

$$\log V = 1.23 \, (\log S - 1)$$

The resulting volumes are 123.2 km^3 in 1963 and 96.3 km^3 in 2001, indicating a loss of 26.9 km^3.

Although they are all highly uncertain, we obtained three independent and consistent measurements for Cook ice cap volume loss between 1963 and 2000, in the range of 25-30 km^3. This is equivalent to an area-average thinning rate of 1.4-1.7 m/yr.

IV. Discussion

IV.1. Climatological context of the glacier retreat

There is only one permanent weather station on Kerguelen Islands. It is located at Port-aux-Français on the eastern and dryer side of the main island, 80 km away from Cook ice cap (Figure 1). Daily values of temperature and precipitation since 1951 are available (Figure 10).

The relationship between the climate at Port-aux-Français and glacier changes must be considered cautiously. First of all, the climate of the Kerguelen Islands is characterized by strong spatial gradients. Rallier du Baty Peninsula and Cook ice cap are part of a north-south mountain range that creates a topographic barrier perpendicular to the dominant westerly winds; they thus receive a large amount of precipitation. Precipitation was measured between 1995 and 2001 in Ampère glacier forefield (source: Institut Paul Emile Victor IPEV 136). The mean annual precipitation was 3155 mm (SD = 300 mm) compared with 692 mm (SD = 160 mm) at Port-aux-Français. On the annual time scale, the two series of precipitation are reasonably well correlated (r^2= 0.39, n=7). For annual temperature, the correlation is good (r^2= 0.83, n=7) and the mean difference is 0.1°C, indicating a more homogenous temperature distribution on Kerguelen Islands.

Careful comparison of climate data and glacier changes is also needed, as the variations in glacier length and area are a delayed response to cumulative climate fluctuations [*Oerlemans*, 2001]. We computed the response time (or volume time scale, Jóhannesson et al. [1989]) of Ampère glacier as the ratio between its characteristic ice thickness (about 300 m [*Vallon*, 1977b]) and the ablation at the terminus (about 10-12 m water equivalent [*Vallon*, 1977a]). A response time of 25-30 years

indicates that Ampère glacier responds quite rapidly to climate perturbations. Note that this response time is representative of one outlet glacier and certainly not of the whole Cook ice cap.
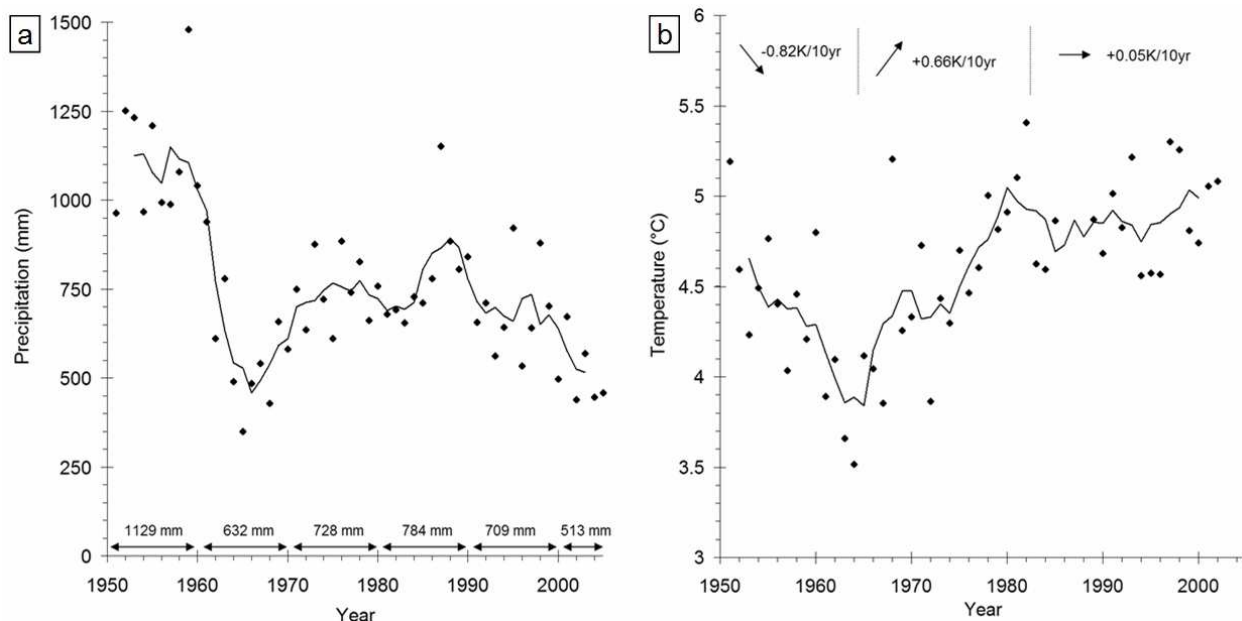

Figure 10: Temperature and precipitation at Port-aux-Français (80 km east of Cook ice cap). The symbols correspond to the yearly values whereas the lines are the 5-year running means. (a) Annual precipitation between 1951 and 2005. The decadal means of precipitation are given above the X-axis. (b) Mean annual temperature between 1951 and 2002. The temperature record has been split into three time periods for which the linear trend is given in the upper part of the graph.

The most striking climate feature is a marked reduction in precipitation in the late 1950s and the early 1960s (Figure 10a). It dropped from 1129 mm in the 1950s to 632 mm in the 1960s. During the accumulation season (April to November on Cook ice cap [*Vallon*, 1977a]), it dropped in the same proportion, from 739 mm to 393 mm. Northward migration of the Antarctic Convergence is a potential candidate that may explain this stepwise shift in climate in the early 1960s [*Hall*, 2002]. Since the 1970s, the annual precipitation remained at a low level, around 700 mm (SD = 150 mm).

The temperature time series can be divided into three periods (Figure 10b). The first [1951-1964] was synchronous with the reduction in precipitation and characterized by decreasing temperature with a trend of -0.82K/10yr. This phase was followed by a period [1965-1981] of rising temperature (+0.66K/10yr). After 1982, the temperature remained at a high level. The linear trend for the 51 year temperature series is a warming of 0.15K/10yr, in agreement with previous work [*Jacka et al.*, 2004]. The warming was similar in spring, summer and fall (0.15-0.2K/10yr) and slightly reduced in winter (0.09K/10yr).

On ice-covered areas, the low level of annual precipitation since the mid-60s and the rise in temperature in the 70s (in particular during the ablation season) have favored negative glacier mass balance by reducing the winter accumulation and lengthening the period of the year in which ice ablation, and not snow ablation, takes place.

IV.2. Factors contributing to the asymmetrical ice wastage

We have observed enhanced ice shrinkage and thinning on the eastern, lee side of Cook ice cap. Similar observations have been in made in South Georgia, where glacier recession on the windward and wetter southwest coast has been less widespread during the second half of the 20th century [*Gordon et al.*, 2008]. The same is true for Heard Island and is attributed to different

climate sensitivity [*Ruddell*, 2006]. In Norway, several maritime glaciers started to advance in the 1990s as a response to higher winter accumulation during the first part of the 1990s [*Chinn et al.*, 2005; *Nesje et al.*, 2008]. The Kerguelen Islands are small and their maritime climate is homogeneous, primarily controlled by the large-scale surface properties of the surrounding Southern Ocean. A differential climate change on both sides of Cook ice cap cannot be excluded but is unlikely as evidenced by the good correlation between the interannual climatic fluctuations at Port-aux-Français and in Ampère glacier forefield. Rather, we will see that differential ice cap sensitivities (changes in terminus properties and hypsometry) may account for the different evolution of its eastern and western sides.

On the eastern side of Cook ice cap, many outlet glacier fronts, which were grounded in 1963, were lake-terminating in 1991 and beyond. The switch from a land- to a water-terminating ice front introduces a calving component into the mass balance of these glaciers and transforms their dynamics and climatic sensitivity [*Kirkbride and Warren*, 1999], generally leading to rapid ice loss [*Chinn*, 1996; *Benn et al.*, 2007; *Larsen et al.*, 2007]. The formation of pro-glacial lakes is an efficient means of eroding a glacier front because of submarine melting due to warm lake waters [*Rohl*, 2006; *Paul et al.*, 2007]. On the western side, only the Pasteur and Pierre Curie glaciers were calving icebergs into the ocean in 1963. Although they experienced a limited retreat, it was enough to transform Pierre Curie glacier into a land-terminating glacier. The switch from a tidewater to a non-calving glacier acts as a stabilizing influence as calving losses are removed.

The hypsometry of Cook ice cap makes it highly sensitive to climate change. Most of the ice cap surface lies between 600 and 900 m a.s.l. (Figure 9). In the 1970s, the equilibrium line altitude was around 700 m a.s.l. [*Vallon*, 1977a], such that even a small change in its altitude leads to major changes in accumulation area ratio and therefore mass balance. This vulnerability, due to the distribution of ice with altitude, differs on the two sides of the ice cap. On the eastern side, 39.5% of the ice cap was below 600 m a.s.l. in 1963, compared to only 26% on the western side. Thus, the ice cap history (prior to 1963) resulted in two different hypsometries that partially controlled its differential wastage.

IV.3. Comparison of glacier changes around the Southern Ocean
As in Kerguelen Islands, the majority of ice masses around the Southern Ocean are rapidly shrinking. This is true at different spatial scales, from a 1.8 km^2 (or 29%) reduction in the area covered by the small Brown glacier on Heard Island (53°S) between 1947 and 2004 [*Thost and Truffer*, 2008] to a 140 km^2 decrease (or 3.4%) for the Northern Patagonian Icefield (NPI, 47°S) between 1975 and 2001 [*Rivera et al.*, 2007]. Changes in ice-covered areas are not reported in South Georgia (54°S) but the majority of glacier fronts are retreating [*Gordon et al.*, 2008]. Area-average thinning rates of about 1 m/yr were observed for the two Patagonian Icefields between 1968/1975 and 2000 [*Rignot et al.*, 2003] and the long term [1947-2004] thinning rate for the Brown glacier is 0.5 m/yr [*Thost and Truffer*, 2008]. We determined higher thinning rates for Cook ice cap, 1.4-1.7 m/yr between 1963 and 2000. The aforementioned studies and our present work consistently point to an accelerated rate of glacier retreat since the 1990s, indicating that these sub-Antarctic glaciers are actively responding to recent changes in climatic conditions.

V. Conclusion

In the present study, we compared historical data and recent data from space-borne sensors to measure the changes in extent and elevation of glaciers and ice caps on the Kerguelen Islands during the last forty-five years. The total ice-covered area on the islands declined from 703 to 552 km^2 between 1963 and 2001. For Cook ice cap, we determined the total volume change between

1963 and 2000 using three independent methods that agreed within ±10%. The ice cap lost 25-30 km^3, equivalent to an area-averaged thinning rate of 1.4-1.7 m/yr. We observed consistently reduced ice loss on the western, windward side of Kerguelen Islands. This asymmetry is mainly attributed to lower mean elevation and the switch from a land- terminating to lake-calving termini for the eastern outlet glaciers.

The accelerated rates of ice loss observed since the 1990s suggest that ice masses on the Kerguelen Islands have not yet approached a steady state. New satellite acquisitions would be useful in assessing whether the apparent trend toward accelerated ice loss is confirmed. A better understanding of the dynamics of glaciers and ice caps on the Kerguelen Islands is also needed in order to predict at what pace they will react to the 1-2°C warming predicted by the end of the 21st century [*Meehl et al.*, 2007].

VI. Acknowledgments

VII. References

Benn, D. I., C. R. Warren, and R. H. Mottram (2007), Calving processes and the dynamics of calving glaciers, *Earth-Science Reviews*, *82*(3-4), 143-179.

Berthier, E., Y. Arnaud, C. Vincent, and F. Remy (2006), Biases of SRTM in high-mountain areas: Implications for the monitoring of glacier volume changes, *Geophysical Research Letters*, *33*(8), L08502.

Carabajal, C. C., and D. J. Harding (2005), ICESat validation of SRTM C-band digital elevation models, *Geophysical Research Letters*, *32*(22), L22S01.

Chinn, T. (1996), New Zealand glacier responses to climate change of the past century, *New Zealand Journal of Geology and Geophysics*, *39*, 415-428.

Chinn, T., S. Winkler, M. J. Salinger, and N. Haakensen (2005), Recent glacier advances in Norway and New Zealand: a comparison of their glaciological and meteorological causes, *Geografiska Annaler*, *87A*(1), 141–157.

Cogley, J. G. (2009), Geodetic and direct mass-balance measurements: comparison and joint analysis, *Annals of Glaciology*, *50*(50), 96-100.

Dall, J., S. N. Madsen, K. Keller, and R. Forsberg (2001), Topography and penetration of the Greenland Ice Sheet measured with airborne SAR interferometry, *Geophysical Research Letters*, *28*(9), 1703-1706.

Durand de Corbiac, H. (1970), La carte de reconnaissance des îles Kerguelen, *Bulletin du Comité National Français des Recherches Antarctiques*, *26*, 1-73.

Dyurgerov, M. B., and M. F. Meier (2005), *Glaciers and the Changing Earth System: a 2004 Snapshot*, 117 pp., INSTAAR, Boulder.

Echelmeyer, K. A., W. D. Harrison, C. F. Larsen, J. Sapiano, J. E. Mitchell, J. DeMallie, B. Rabus, G. Adalgeirsdottir, and L. Sombardier (1996), Airborne surface profiling of glaciers: A case-study in Alaska, *Journal of Glaciology*, *42*(142), 538-547.

Frenot, Y., J.-C. Gloaguen, G. Picot, J. Bougère, and D. Benjamin (1993), *Azorella selago* Hook. used to estimate glacier fluctuations and climatic history in the Kerguelen Islands over the last two centuries, *Oecologia*, *95*, 140-144.

Gordon, J. E., V. M. Haynes, and A. Hubbard (2008), Recent glacier changes and climate trends on South Georgia, *Global and Planetary Change*, *60*(1-2), 72-84.

Hall, K. (2002), Review of Present and Quaternary periglacial processes and landforms of the maritime and sub-Antarctic region, *South African Journal of Science*, *98*(1-2), 71-81.

Institut Géographique National (1967), Carte de reconnaissance, 1:200,000, Vincennes, France.

Jacka, T. H., W. F. Budd, and A. Holder (2004), A further assessment of surface temperature changes at stations in the Antarctic and Southern Ocean, 1949-2002, *Annals of Glaciology*, *29*, 331-338.

Johannesson, T., C. Raymond, and E. D. Waddington (1989), Time-scale for adjustment of glaciers to changes in mass balance, *Journal of Glaciology*, *35*(121), 355-369.

Kirkbride, M. P., and C. R. Warren (1999), Tasman Glacier, New Zealand: 20th-century thinning and predicted calving retreat, *Global and Planetary Change*, *22*(1-4), 11-28.

Larsen, C. F., R. J. Motyka, A. A. Arendt, K. A. Echelmeyer, and P. E. Geissler (2007), Glacier changes in southeast Alaska and northwest British Columbia and contribution to sea level rise, *Journal of Geophysical Research-Earth Surface*, *112*(F1), F01007.

Leprince, S., S. Barbot, F. Ayoub, and J. P. Avouac (2007), Automatic and Precise Orthorectification, Coregistration, and Subpixel Correlation of Satellite Images, Application to Ground Deformation Measurements, *IEEE Transactions on Geoscience and Remote Sensing*, *45*(6), 1529-1557.

Meehl, G. A., T. F. Stocker, W. D. Collins, P. Friedlingstein, A. T. Gaye, J. M. Gregory, A. Kitoh, R. Knutti, J. M. Murphy, A. Noda, S. C. B. Raper, I. G. Watterson, A. J. Weaver, and Z.-C. Zhao (2007), Global Climate Projections, in *Climate Change 2007: The Physical Science Basis. Contribution of Working Group I to the Fourth Assessment Report of the Intergovernmental Panel on Climate Change*, edited by S. Solomon, et al., pp. 747-845, Cambridge University Press, Cambridge, United Kingdom and New York, NY, USA.

Nesje, A., J. Bakke, S. O. Dahl, O. Lie, and J. A. Matthews (2008), Norwegian mountain glaciers in the past, present and future, *Global and Planetary Change*, *60*(1-2), 10-27.

Oerlemans, J. (2001), *Glaciers and climate change*, A. A. Balkema Publishers, Rotterdam.

Paterson, W. S. B. (1972), Laurentide Ice Sheet: estimated volumes during late Wisconsin, *Reviews of Geophysics and Space Physics*, *10*, 885-917.

Paul, F., A. Kaab, and W. Haeberli (2007), Recent glacier changes in the Alps observed by satellite: Consequences for future monitoring strategies, *Global and Planetary Change*, *56*(1-2), 111-122.

Poggi, A. (1977), Heat balance in the ablation area of the Ampere Glacier (Kerguelen Islands), *Journal of Applied Meteorology*, *16*, 48-55.

Rabus, B., M. Eineder, A. Roth, and R. Bamler (2003), The shuttle radar topography mission - a new class of digital elevation models acquired by spaceborne radar, *ISPRS Journal of Photogrammetry and Remote Sensing*, *57*(4), 241-262.

Raup, B., A. Kääb, J. S. Kargel, M. P. Bishop, G. Hamilton, E. Lee, F. Paul, F. Rau, D. Soltesz, S. J. S. Khalsa, M. Beedle, and C. Helm (2007), Remote sensing and GIS technology in the Global Land Ice Measurements from Space (GLIMS) project, *Computers & Geosciences*, *33*(1), 104-125.

Rignot, E., K. Echelmeyer, and W. Krabill (2001), Penetration depth of interferometric synthetic-aperture radar signals in snow and ice, *Geophysical Research Letters*, *28*(18), 3501-3504.

Rignot, E., A. Rivera, and G. Casassa (2003), Contribution of the Patagonia Icefields of South America to sea level rise, *Science*, *302*(5644), 434-437.

Rivera, A., T. Benham, G. Casassa, J. Bamber, and J. A. Dowdeswell (2007), Ice elevation and areal changes of glaciers from the Northern Patagonia Icefield, Chile, *Global and Planetary Change*, *59*(1-4), 126-137.

Rodriguez, E., C. S. Morris, and J. E. Belz (2006), A global assessment of the SRTM performance, *Photogrammetric Engineering and Remote Sensing*, *72*(3), 249-260.

Rohl, K. (2006), Thermo-erosional notch development at fresh-water-calving Tasman Glacier, New Zealand, *Journal of Glaciology*, *52*(177), 203-213.

Ruddell, A. (2006), An inventory of present glaciers on Heard Island and their historical variation, in *Heard Island: Southern ocean sentinel*, edited by K. Green and E. Whoehler, pp. 28-51, Surrey Beatty and Sons, Chipping Norton.

Surazakov, A. B., and V. B. Aizen (2006), Estimating volume change of mountain glaciers using SRTM and map-based topographic data, *IEEE Transactions on Geoscience and Remote Sensing*, *44*(10), 2991-2995.

Thost, D. E., and M. Truffer (2008), Glacier Recession on Heard Island, Southern Indian Ocean, *Arctic, Antarctic and Alpine Research*, *40*(1), 199-214.

Vallon, M. (1977a), Bilan de masse et fluctuations récentes du Glacier Ampère (Iles Kerguelen, TAAF), *Zeitschrift für Gletscherkunde und Glazialgeologie*, *13*, 55-85.

Vallon, M. (1977b), Topographie sous glaciaire du Glacier Ampère (Iles Kerguelen, TAAF), *Zeitschrift für Gletscherkunde und Glazialgeologie*, *13*, 37-55.

Zwally, H. J., B. Schutz, W. Abdalati, J. Abshire, C. Bentley, A. Brenner, J. Bufton, J. Dezio, D. Hancock, D. Harding, T. Herring, B. Minster, K. Quinn, S. Palm, J. Spinhirne, and R. Thomas (2002), ICESat's laser measurements of polar ice, atmosphere, ocean, and land, *Journal of Geodynamics*, *34*(3-4), 405-445.